Mott-Insulator Transition in a Two-Dimensional Atomic Bose Gas

I. B. Spielman,* W. D. Phillips, and J. V. Porto

Joint Quantum Institute, National Institute of Standards and Technology, and University of Maryland, Gaithersburg, Maryland, 20899, USA

(Received 23 October 2006; published 22 February 2007)

Cold atoms in periodic potentials are versatile quantum systems for implementing simple models prevalent in condensed matter theory. Here we realize the 2D Bose-Hubbard model by loading a Bose-Einstein condensate into an optical lattice, and study the resulting Mott insulator. The measured momentum distributions agree quantitatively with theory (no adjustable parameters). In these systems, the Mott insulator forms in a spatially discrete shell structure which we probe by focusing on correlations in atom shot noise. These correlations show a marked dependence on the lattice depth, consistent with the changing size of the insulating shell expected from simple arguments.

DOI: 10.1103/PhysRevLett.98.080404 PACS numbers: 05.30.Jp, 03.75.Hh, 03.75.Lm

In recent years, ultracold atoms confined in optical lattices have realized strongly interacting condensed matter phenomena, including the Girardeau-Tonks gas in 1D [1,2] and the superfluid to Mott-insulator transition in 3D, and 1D [3,4]. While the existence of a 2D Mott insulator has been verified in the cold atom system [5], it has gone largely unexplored. 2D interacting Bose systems represent an interesting middle ground between 1D and 3D; quantum fluctuations are essential, as in 1D, destroying Bose condensation, but 2D systems still exhibit superfluity, as in 3D [6,7]. The atom-optical system differs substantially from traditional condensed matter systems both in control (the trapping potentials can be changed dynamically on all relevant experimental time scales) and in measurement opportunities (e.g., imaging after time of flight provides a direct measurement of the momentum distribution). These techniques allow us to study the 2D Mott-insulator via its momentum distribution and correlations in its noise [8–11]. We present momentum distributions which quantitatively agree with the predictions of a 2D theory with no adjustable parameters (even approaching the insulator-superfluid transition, where perturbation theory breaks down). In the cold atom system, the transition from superfluid to insulator occurs smoothly; the system segregates into shell-like domain(s) of insulator and superfluid [12–15]. We detect signatures of an insulating shell via correlations in atom shot noise; in our data these correlations behave as expected due to the changing size of the Mott-insulator region.

We realize an ensemble of 2D Bose systems in a combined sinusoidal plus harmonic potential. Absent the harmonic confinement, the system is well described by the Bose-Hubbard (B-H) Hamiltonian [12,16], with a matrix element for tunneling between sites t and an on-site energy cost for double occupancy U. The ground state is either a superfluid (SF) or a Mott insulator (MI). For unit filling (on average one atom per lattice site), the 2D B-H system exhibits a zero temperature quantum phase transition from SF to MI [16] when the ratio $t/U \approx 0.06$ [17,18], which we denote by $(t/U)_c$. When $t/U = 0$, the unit filled MI has exactly one atom per lattice site. At finite t/U variations from unit occupation are correlated between nearby sites, giving a momentum distribution with broad, diffractive, structure [19].

Harmonic confinement modifies the physics from the homogenous case. This can be modeled in terms of a ''local chemical potential'' varying from a peak value in the center of the trap to zero at the edges (a local density approximation, LDA). As t/U decreases, domains of MI separated by SF grow continuously, forming a discrete shell structure [12–15]. In our experiment, we expect shells of SF and unit-occupancy MI.

We prepare a B-H at a specific value of t/U (calculated from the 2D band structure), measure the momentum distribution, and extract correlations in its noise. The loss of diffraction in the momentum distribution [3] as the system progresses through the Mott regime is shown in Fig. . Because of the MI shell structure, it can be difficult to deconvolve the separate contributions to the data, particularly near $(t/U)_c$. However, we find that a theory for the homogeneous system is surprisingly good at describing the momentum distribution.

Figure 1(b) shows momentum noise correlations, where diffractive structure persists deep into the Mott regime [8,9]. In this limit, the width of the correlation peaks should be diffraction limited by the inverse linear size of the Mott domain, and the integrated signal of the correlation peaks should depend on the number of occupied lattice sites in the MI. Indeed, we observe the ''area'' A of the correlation peaks increases with increasing t/U.

We produce nearly pure 3D ^{87}Rb BECs with $N_T = 1.7(5) \times 10^5$ [20] atoms in the $|F = 1, m_F = -1\rangle$ state [21]. The BEC is separated in 200 ms into an array of about 60 2D systems by an optical lattice aligned along $\hat{z}$ (vertical lattice). This lattice is formed by a pair of linearly polarized $\lambda = 820$ nm laser beams [22]. A square lattice in the $\hat{x}$-$\hat{y}$ plane is produced by a beam in a folded-retroreflected configuration linearly polarized in the $\hat{x}$-$\hat{y}$ plane [23]. This $\hat{x}$-$\hat{y}$ lattice is applied in 100 ms [24]. The intensities of the vertical and x-y lattices start at zero,

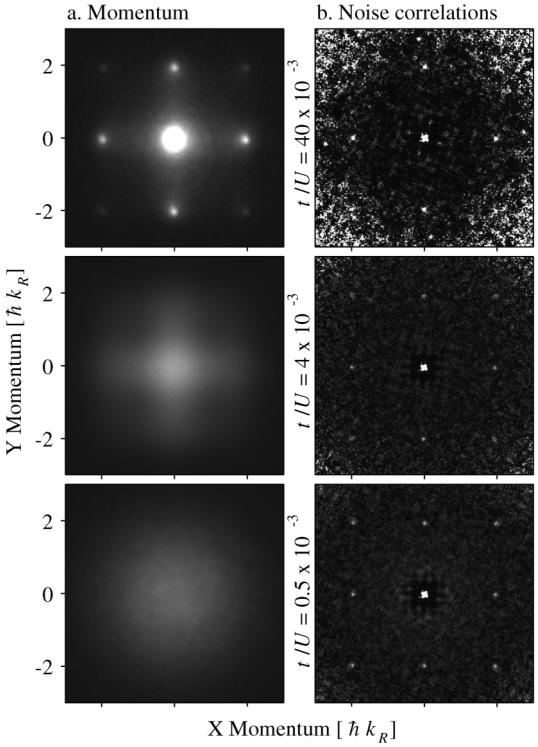

FIG. 1. Results at three values of t/U: 40×10^{-3}, 4×10^{-3}, and 0.5×10^{-3}. (a) Atom density versus momentum. (b) Noise correlations versus momentum difference. Each displayed image was averaged from ≈ 60 raw images; to reduce technical noise, the displayed correlation data was averaged with itself, rotated by 90°.

follow exponentially increasing ramps (with 50 and 25 ms time constants, respectively), and reach their peak values simultaneously. These time scales are chosen to be adiabatic with respect to mean-field interactions, vibrational excitations, and tunneling within each 2D system [25]. The final depth of the $\hat{x}$-$\hat{y}$ lattice determines t/U and ranges from $V = 0$ to $31(2)E_R$, and the final vertical lattice depth is $30(2)E_R$ (where $E_R = \hbar^2 k_R^2/2m = h \times 3.4$ kHz and $k_R = 2\pi/\lambda$). We measure lattice depths by pulsing the lattice for 3 μs and observing the resulting atom diffraction [26].

As prepared, the system is a stack of 2D Bose gases each in a square lattice of depth V and at a typical density of 1 atom per site. The atoms are held for 30 ms; then all confining potentials are abruptly removed (the lattice and magnetic potentials turn off in $\lesssim 1$ μs and $\simeq 300$ μs, respectively). This projects the initial states onto free particle states which expand for 20 to 30 ms, and are then detected by resonant absorption imaging [27]. Because initial momentum maps into final position, an image measures the 2D momentum distribution $n(k_x, k_y)$, which we average over many realizations.

Figure 1(a) shows a series of such averages, starting near the SF-MI transition and crossing deep into the MI phase [3]. These data smoothly progress from sharp diffraction peaks on a small background (top), and culminates with a nearly-perfect Gaussian (bottom). Because of shell structure, the diffraction images can be difficult to interpret, returning to simplicity in the limits of shallow or deep lattices where the system consists of just SF or MI.

When $t/U = 0$, the MI has an exact number of atoms in each occupied site, in our case $n = 1$. For small t/U, the unit-occupied state is modified to first order in perturbation theory with a small mixture of neighboring particle-hole pairs. This gives a modulated momentum distribution: $\langle \hat{n}_k \rangle = N|w(\mathbf{k})|^2\{1 + \alpha[\cos(\pi k_x/k_R) + \cos(\pi k_y/k_R)]\}$ [19]. Here $\alpha = 8t/U$, and $w(\mathbf{k})$ is the Fourier transform of the Wannier states in the lattice sites; $w(\mathbf{k})$ is well approximated by a Gaussian for the data described here. [As the density modulations result from an interference between the unit-occupied Mott state and the particle-hole admixture, the lowest order correction is $\langle \hat{n}_k \rangle \propto t/U$, while the probability for double occupancy scales as $(t/U)^2$.] In 3D, the first order dependence $\alpha \propto t/U$ was verified over a range of parameters [19]. Agreement near the MI-SF transition can be surprising for two reasons: (1) only a fraction of the inhomogeneous system may be in the MI phase; (2) as t/U increases, higher order contributions become important.

To quantify these terms, we expand an analytic result [28] to order $(t/U)^2$, correcting the momentum distribution by $72(t/U)^2[\cos(\pi k_x/k_R) + \cos(\pi k_y/k_R)]^2$. This yields Fourier terms $\beta_1[\cos(2\pi k_x/k_R) + \cos(2\pi k_y/k_R)]$, and $\beta_2 \cos(\pi k_x/k_R)\cos(\pi k_y/k_R)$; we define the average coefficient $\beta = (\beta_1 + \beta_2)/2 = 90(t/U)^2$. (Terms higher order in t/U also contribute slightly to β_1 and β_2.)

Measured coefficients α and β (from Fourier transformed quasimomentum distributions, computed as described below) are plotted in Fig. 2. The dashed lines are the predictions: $\alpha = 8t/U$ and $\beta = 90(t/U)^2$ (no adjust-

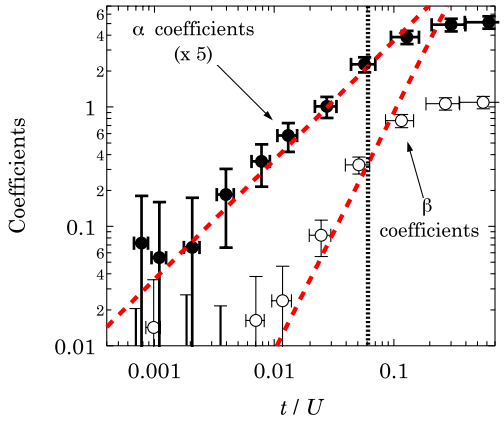

FIG. 2 (color online). Solid symbols: measured first order coefficient α versus t/U. The overlayed red (or gray) dashed line shows the prediction, $\alpha = 8t/U$. (These data and the fit have been displaced for clarity: vertically as indicated, and by about 2% horizontally.) Empty symbols: averaged second order coefficient β versus t/U. The associated red (or gray) dashed line is the prediction, $\beta = 90(t/U)^2$. The vertical dotted line indicates the expected location of the 2D SF-MI transition [17,18].

able parameters). The vertical black line denotes $(t/U)_c = 0.06$, where we expect the MI to first nucleate in our sample. Points to the left of the black dotted line (MI regime) agree with expectations. Near the MI transition the first and second order terms become comparable, indicating the incipient breakdown of perturbation theory.

In Fig. 3 we compare the measured quasimomentum distribution with theory (solid lines). The momentum distribution is the product of the magnitude squared Wannier function $|\omega(k)|^2$ and $\langle \hat{n}_q \rangle$ (periodic along $\hat{x}$ and $\hat{y}$ in the reciprocal lattice vectors, $2k_R$). To extract the normalized quasimomentum distribution we divide the data by $|\omega(k)|^2$, then normalize a properly weighted average of all points separated by multiples of reciprocal lattice vectors. At small t/U, the quasimomentum distribution is cosinusoidal. As t/U increases toward $(t/U)_c$, contributions of higher Fourier terms become important, as is evident in the cross section at $t/U = 25 \times 10^{-3}$ and the coefficients of Fig. 2. The shape of the measured distribution matches the predictions of theory with no free parameters.

A homogeneous-system theory provides a remarkably good representation of the data discussed above. This results from two facts: except quite close to the MI transition, nearly all of the system should be unit-occupied MI; and by focusing only on the largest momentum scales (corresponding to spatial length scales on the order of 1 or two lattice sites) we are insensitive to the size of the MI. However, the size of the MI almost exclusively determines the area and width of the peaks in the noise-correlations signal [Fig. 1(b)] [8,9,29].

We determine noise correlations from our images of atom density $n(k_x, k_y)$ by computing the autocorrelation function (ACF) averaged over many images: $S(\delta k_x, \delta k_y) = \langle \int n(k_x, k_y) n(k_x + \delta k_x, k_y + \delta k_y) dk_x dk_y \rangle$. To compare with theory, we normalize by the ACF of the average, $S_0(\delta k_x, \delta k_y) = \int \langle n(k_x, k_y) \rangle \langle n(k_x + \delta k_x, k_y + \delta k_y) \rangle dk_x dk_y$; i.e., we determine $S(\delta k_x, \delta k_y)$ by calculating the ACF of each image separately, and then average over many realizations, typically (40 to 80). [Normalizing by the S_0 removes the dependence of $S(\delta k_x, \delta k_y)$ on the momentum distribution $\langle n(k_x, k_y) \rangle$.] Deep in the MI phase, $S(\delta k_x, \delta k_y)$ has diffractive structure, with noise correlation peaks separated by $2k_R$, revealing the underlying lattice structure.

In the limit of a deep lattice, the ground state of our system is a 3D array of lattice sites with exactly one atom per site. As is usual for diffraction phenomena, δ is determined by the size of the array, and is proportional to L^{-1}, where $L \propto N^{1/3}$ is the linear extent of the MI region and N is the number of sources (lattice sites). Likewise, A is related to the atom number in the MI by $A = (2k_R)^2/N$ [9]. As with most noise, the noise-correlation variance scales as N. We normalize by a quantity which scales like $1/N^2$, so the relative fluctuations described by A have an overall $1/N$ dependence. We calculate that this remains true including order t/U corrections to the MI state. [Order $(t/U)^2$ terms, which we have not investigated, may alter this behavior.]

As the system approaches $(t/U)_c$ from below, we expect the size of the MI region to shrink, and correspondingly for δ and A to increase (the total number of atoms in the experiment N_T remains fixed; only the number of atoms in the MI N decreases). Figure 4 shows this general behavior. Our study of the noise correlations near the MI critical point is enabled by a masking procedure: in each image we eliminate regions of radius 35 μm $\approx 0.3 \times k_R$ centered on the diffraction peaks before computing corre-

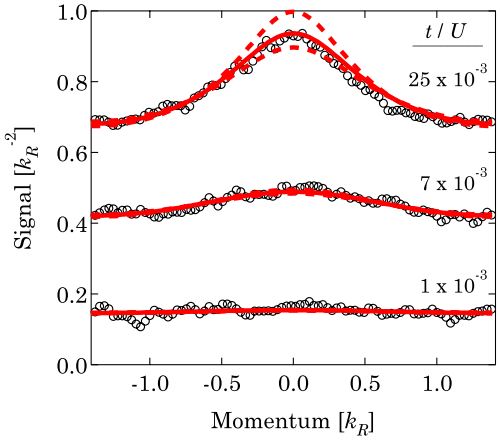

FIG. 3 (color online). Cross sections of normalized quasimomentum distributions (along $\hat{x} + \hat{y}$, and offset for clarity) at three values of t/U. The data are plotted along with the theoretical profile (solid lines) [28]. The dashed lines (not visible in the bottom trace) reflect the uncertainty in the theory resulting from the single-shot $\pm 0.5 E_R$ uncertainty in the lattice depth.

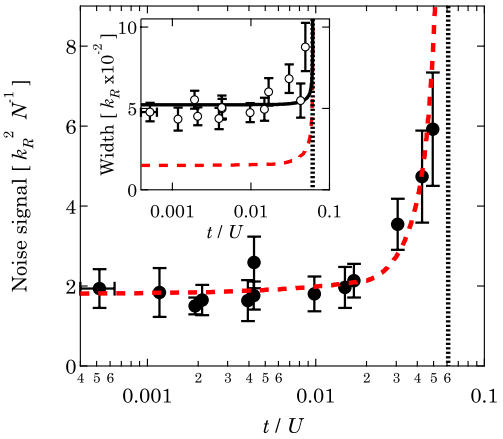

FIG. 4 (color online). Average area of the noise-correlation peaks expressed in units of k_R^2/N_T. The dashed line, denoting A as calculated in our LDA model, was scaled by 0.45 to lie upon the data (see text). Inset: the solid symbols indicate the measured peak width, δ, in units of k_R. The dashed line is the expected width from our LDA computation. The solid line shows the modeled δ including the imaging resolution [27] of $0.05 k_R$. In both cases, the vertical dotted line shows the expected location of the 2D SF-MI transition [17,18], and the uncertainties reflect the statistical uncertainty of the fit due to background noise.

lation functions. This removes spurious effects of the sharp diffraction peaks at larger t/U; tests found no systematic errors associated with our masking procedure [27]. (Fölling *et al.* used a similar technique, but only deep in the MI phase, to show that the correlation peaks do not result from spurious effects of remnant diffraction [9].)

Figure 4 shows A measured by fitting the peaks to 2D Gaussians. A increases with t/U, indicating that the fraction of the system in the MI state is decreasing as expected. A is expected to be $(2k_R)^2/N_T$ for small t/U; however, our data tend to about 45% of this (a similar suppression of the noise signal was observed in Ref. [9]). We attribute at least some of this discrepancy to collisions during the ballistic expansion of the system, which modify some atoms' trajectories, removing those atoms from the correlation features; errors in number calibration could also contribute.

The data are plotted along with a dashed line showing the expected area due to the finite size of the Mott domain, which we calculated in a LDA using a 2D MI phase diagram [17]. After scaling the model by a factor of 0.45, it agrees to within our uncertainties.

The width δ is shown as an inset to Fig. 4; the symbols are the measured RMS peak widths from a Gaussian fit, and the dashed line is the expected peak width for a pure MI with size given by our LDA model. At small t/U, the data saturate to about $0.045k_R$, compared with the $0.015k_R$ expected in our model. This saturation is due to at least two effects: (1) the finite resolution of our optical system [27], and (2) the ~ 15 μm initial radius of the sample. We estimate that each of these effects would separately limit the measured peak width to about 0.03 and $0.04k_R$, respectively. (The width may also be influenced by mean field during expansion.) The black dashed line shows the modeled δ added in quadrature with the terms described above.

In our simple calculation (valid to first order in t/U), A and δ depend only on the size of the Mott domain. More sophisticated theoretical techniques can be applied to this problem, indeed explicit numerical calculations for a harmonically confined 1D and 2D systems exist [29,30]. These results agree qualitatively with our data, and further measurements near the MI transition could quantitatively test these calculations.

In this Letter we demonstrate a remarkable agreement between experiment and theory describing the momentum distribution of a 2D MI over a wide range of conditions, and to second order in perturbation theory. Additionally, we see that correlations in the atom shot noise yield information about the fraction of the system in the MI. Even when the momentum distribution is featureless, the noise correlations show the lattice structure and indicate system size. This adds support to proposals to identify the phases of extended B-H models (including a possible supersolid phase), using a combination of momentum and noise-correlation measurements [30].

We would like to thank V. W. Scarola, E. Demler, A. M. Rey, and C. Williams for delightful conversations, M. Anderlini and J. Sebby-Strabley for lattice setup. This work was partially supported by ARDA/DTO, and ONR; I. B. S. thanks the NIST/NRC postdoctoral program.

*Electronic address: ian.spielman@nist.gov

[1] B. Paredes *et al.*, Nature (London) **429**, 277 (2004).
[2] T. Kinoshita, T. R. Wenger, and D. S. Weiss, Science **305**, 1125 (2004).
[3] M. Greiner *et al.*, Nature (London) **415**, 39 (2002).
[4] T. Stöferle *et al.*, Phys. Rev. Lett. **92**, 130403 (2004).
[5] M. Köhl *et al.*, J. Low Temp. Phys. **138**, 635 (2005).
[6] V. L. Berezinskii, Sov. Phys. JETP **34**, 610 (1972).
[7] J. M. Kosterlitz and D. J. Thouless, J. Phys. C **5**, L124 (1972).
[8] E. Altman, E. Demler, and M. D. Lukin, Phys. Rev. A **70**, 013603 (2004).
[9] S. Fölling *et al.*, Nature (London) **434**, 481 (2005).
[10] M. Greiner, C. A. Regal, J. T. Stewart, and D. S. Jin, Phys. Rev. Lett. **94**, 110401 (2005).
[11] M. Schellekens *et al.*, Science **310**, 648 (2005).
[12] D. Jaksch *et al.*, Phys. Rev. Lett. **81**, 3108 (1998).
[13] G. G. Batrouni *et al.*, Phys. Rev. Lett. **89**, 117203 (2002).
[14] S. Fölling *et al.*, cond-mat/0606592.
[15] G. K. Campbell *et al.*, cond-mat/0606642.
[16] M. P. A. Fisher, P. B. Weichman, G. Grinstein, and D. S. Fisher, Phys. Rev. B **40**, 546 (1989).
[17] N. Elstner and H. Monien, cond-mat/9905367.
[18] S. Wessel, F. Alet, M. Troyer, and G. G. Batrouni, Phys. Rev. A **70**, 053615 (2004).
[19] F. Gerbier *et al.*, Phys. Rev. Lett. **95**, 050404 (2005); Phys. Rev. A **72**, 053606 (2005).
[20] All uncertainties herein reflect the uncorrelated combination of single-sigma statistical and systematic uncertainties.
[21] I. B. Spielman *et al.*, Phys. Rev. A **73**, 020702(R) (2006).
[22] We replicated these experiments with our laser tuned to 810 nm. Our results for the noise-correlation measurements include both data sets.
[23] J. Sebby-Strabley, M. Anderlini, P. S. Jessen, and J. V. Porto, Phys. Rev. A **73**, 033605 (2006).
[24] The vertical lattice beams intersect at $\theta = 162(1)^\circ$ giving a lattice period of 415(1) nm. The beams for vertical and $\hat{x}$-$\hat{y}$ lattices differ in frequency by ≈ 80 MHz.
[25] The vertical lattice loading is adiabatic with respect to tunneling, giving a final ensemble of 2D systems whose respective phases are randomized. While we do not know the temperature in the lattice, we begin with a nearly pure BEC and are confident that our loading procedure does not cause excessive heating. To check this, we created a MI as described in the text, then decreased the lattice potential in about 30 ms, verifying the reappearance of sharp diffraction orders.
[26] Y. B. Ovchinnikov *et al.*, Phys. Rev. Lett. **83**, 284 (1999).
[27] For complete technical details of the analysis refer to I. B. Spielman, W. D. Phillips, and J. V. Porto, cond-mat/0606216.
[28] K. Sengupta and N. Dupuis, Phys. Rev. A **71**, 033629 (2005).
[29] A. M. Rey, I. I. Satija, and C. W. Clark, cond-mat/0511700.
[30] V. W. Scarola, E. Demler, and S. D. Sarma, Phys. Rev. A **73**, 051601(R) (2006).